Coarse-Grained Molecular Dynamics Study of Cyclic Peptide Nanotube Insertion into a Lipid Bilayer†

Hyonseok Hwang*

Department of Chemistry and Institute for Molecular Science and Fusion Technology, Kangwon National University, Chuncheon, Kangwon 200-701, Republic of Korea

George C. Schatz and Mark A. Ratner

Department of Chemistry, Northwestern University, 2145 Sheridan Road, Evanston, Illinois 60208-3113

Received: September 11, 2008

Coarse-grained (CG) molecular dynamics (MD) simulations are performed to study the insertion of cyclic peptide nanotubes into cell membranes and to examine whether cyclic peptide nanotubes can function as an ion channel and thereby as an antibacterial agent. To do so, the two coarse-grained (CG) models for lipid molecules and for proteins developed by Marrink et al. (*J. Phys. Chem. B* **2004**, *108*, 750) and by Shih et al. (*J. Phys. Chem. B* **2006**, *110*, 3674), respectively, were extended and modified. These CG models were verified by performing CG MD and all-atom (AA) MD simulations for a cyclic peptide nanotube, 8 × cyclo[(−D-Ala-L-Glu-D-Ala-L-Gln−)$_2$], in water and by comparing the results from the two simulations. Comparison between static and dynamic (water transport) properties obtained from both simulations shows good agreement. To study nanotube insertion, a CG cyclic peptide nanotube, 8 × cyclo[(−Trp-D-Leu−)$_4$], was prepared above the surface of a CG DPPC lipid bilayer, restrained with constraints, and equilibrated, and then a series of CG MD simulations were carried out by lifting the constraints imposed on the nanotube. The CG MD simulations show that the cyclic peptide nanotube spontaneously inserts into and reorients inside the lipid bilayer. After insertion, the long axis of the cyclic peptide nanotube is aligned approximately perpendicular to the bilayer plane indicating that the nanotube can function as an ion channel and as an antibacterial agent. Tilt structures of the cyclic peptide nanotubes inside the lipid bilayer are found to be in agreement with experiment and earlier AA simulations. Lipid flip-flop, a migration of lipid molecules from one leaflet to the other leaflet of the lipid bilayer, is also observed from the CG MD simulations. Finally, the CG MD simulations reveal that a lipid headgroup can be inserted into the cyclic peptide nanotube. This process is confirmed by an AA MD simulation.

I. Introduction

Cyclic peptide nanotubes are a class of synthetic proteins, functioning as an ion channel.[1−7] They are formed from closed peptide rings, each having an even number of alternating D- and L-amino acid residues. When the cyclic peptide rings are stacked on top of each other through hydrogen bonding, a tubular structure is produced. The cyclic peptide nanotubes in general fall into two categories: one with hydrophilic side chains and the other with hydrophobic side chains (see Figure 1).[1,2] As a result, depending on the nature of the side chains, they can be found either in water solution or in lipid bilayers.

Cyclic peptide nanotubes having hydrophobic side chains draw more attention than those with hydrophilic side chains because the hydrophobic nature of the side chains drives the nanotubes to embed into biological membranes. Fernandez-Lopez et al. showed in an experiment that cyclic peptide nanotubes with hydrophobic side chains can be used as an antibacterial agent.[8,9] In their experiment, mice were infected with a lethal dose of bacteria and then treated with a dose of cyclic peptide nanotubes. Compared with that of untreated mice, the survival probability of the groups of treated mice was much higher, suggesting that the cyclic peptide nanotubes act on bacterial cell membranes, increase membrane permeability to ions, collapse the transmembrane ion potential, and finally cause rapid bacterial cell death.

Whether or not the cyclic peptide nanotubes function as an antibacterial agent depends on how they insert into cell membranes and what is the final structure inside cell membranes. If the nanotube is aligned parallel to the normal axis of the cell membranes after insertion, the nanotubes will function as an ion channel, and thereby as an antibacterial agent. If other structures of the nanotubes after insertion turn out to be more likely, then other pathways must exist for the nanotube to function as an antibacterial agent. Consequently, it is important to study both the insertion of cyclic peptide nanotubes into cell membranes and their subsequent structures inside the membranes.

The all-atom (AA) or atomistic molecular dynamics (MD) simulation method is a useful tool with which to investigate processes in biological systems because the method provides atomistic details of the processes.[10−14] One challenge associated with the AA MD simulation method is that it requires significant computational resources due to the time and length scales involved in biological systems. Although considerable advance has been made in computing power, AA MD simulations are still computationally demanding for many processes.

† Part of the "George C. Schatz Festschrift".

* To whom correspondence should be addressed. E-mail: hhwang@kangwon.ac.kr.

10.1021/jp8080657 CCC: $40.75
Published on Web 11/26/2008

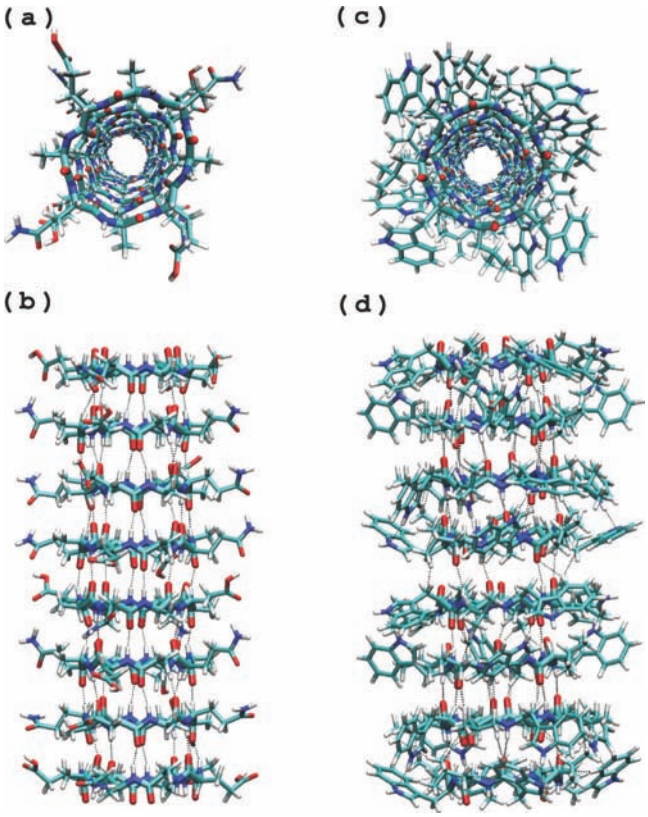

Figure 1. (a, c) Top views and (b, d) side views of cyclic peptide nanotubes, $8 \times$ cyclo[(−D-Ala-L-Glu-D-Ala-L-Gln−)$_2$] and $8 \times$ cyclo[(−L-Trp-D-Leu−)$_4$], respectively. Hydrogen bonds between the cyclic peptide rings are represented by dotted lines.

Coarse-grained (CG) MD simulations provide an alternative to the AA MD simulation method.[15−34] Coarse-grained (CG) modeling, in which a small group of atoms is represented by a single CG bead, reduces the overall system size compared to AA modeling, leading to a significant increase in the computational efficiency of MD simulations. As a result, this approach allows us to explore large biological systems such as proteins in cell membranes.[21,31,33−35] Klein and et al. developed a CG model to describe self-assembly of lipid molecules and extended the model to elucidate the fundamental mechanism of membrane insertion of a model peptide nanotube.[15,16,19−22] A mixed all-atom and coarse-grained (AA-CG) model of the gramicidin A (gA) ion channel embedded in a DMPC lipid bilayer was built by Voth and co-workers.[24,25,33] In this model, the gA peptide was described in full atomistic detail, while the lipid and water molecules were described using a CG model. Marrink et al. also developed force fields for a CG model to depict various structures of lipid molecules and recently refined and extended the force fields for proteins.[18,34] Shih and co-workers extended the CG force field for lipid molecules from Marrink et al. to investigate lipoprotein assembly.[29,30]

In this study, we use a CG model for MD simulations to investigate insertion of cyclic peptide nanotubes into a DPPC lipid bilayer and we characterize the nanotube structure inside a bilayer. For lipid molecules, we adopt the CG model developed by Marrink et al., and for cyclic peptide nanotubes, we modify and extend the CG model by Shih and co-workers. To verify the modified CG force field for cyclic peptide nanotubes, we perform both AA MD and CG MD simulations for a cyclic peptide nanotube in water and compare the results from both simulations. We then carry out CG MD simulations by placing a CG cyclic peptide nanotube above a CG DPPC lipid bilayer and by allowing it to move freely. We believe that the current study will provide useful insight for understanding the membrane insertion process of cyclic peptide nanotubes and for interpreting the experimental results. This CG MD simulation study will also shed light on insertion mechanisms of other proteins into cell membranes.

TABLE 1: Protein Residues, CG Bead Types, and Bond Lengths between Backbone and Side Chain Beads for Cyclic Peptide Nanotubes

residue	CG bead type	equilibrium bond length (Å)
ALA	C	1.5
GLU	Nda	4.0
GLN	Nda	4.0
LEU	C	3.5
TRP	C	4.5

This article is organized as follows. In the next section, we introduce a CG model we use for MD simulations. We also describe the systems we will explore. In section III, simulation results are presented, and discussion and conclusions are made in the final section. Further work and studies are also presented in the final section.

II. Simulation Methods

A. Potential Energy Functions and Force Fields for the Lipid Molecules and Cyclic Peptide Nanotubes. We modified and extended the CG models from Marrink et al. for lipids and from Shih et al. for proteins to describe the structure and dynamics of the cyclic peptide nanotubes.[18,29,30] For the bonded and nonbonded interactions for the lipid and water model, we use the CG model identical to that developed by Marrink and co-workers.[18] In this model, each CG bead is classified into four types: polar (P), nonpolar (N), apolar (C), and charged (Q). The nonpolar and charged beads are further distinguished by their hydrogen bonding capabilities: no hydrogen bond (0), hydrogen bond donor (d), hydrogen bond acceptor (a), and both hydrogen bond donor and acceptor (da). Since detailed explanations of the force field are elsewhere,[18] we do not provide further details here.

For the CG modeling of the cyclic peptide nanotube, each amino acid residue is mapped onto two CG beads according to the CG model of Shih et al.[29,30] Thereby, there are 16 beads in total for each cyclic peptide ring composed of eight amino acids. These include eight beads representing the backbones of the ring with type Nda and eight beads representing the side chains whose types vary. Table 1 shows the protein residues, CG bead types, and equilibrium bond lengths between the backbone and side chain beads in our simulations.

Bonded interactions between two connected beads i and j in the CG nanotubes are described by a harmonic potential and are given by

$$V_{ij}^{\text{bond}}(R) = \frac{1}{2} K_{ij}^{\text{bond}} (R - R_{ij}^{\text{eq}})^2 \quad (1)$$

where R, K_{ij}, and R_{ij}^{eq} are the distance, force constant, and equilibrium bond length between two bonded beads i and j, respectively. The values of the parameters for the bonded interaction are $K_{ij}^{\text{bond}} = 1250$ kJ mol^{-1} nm^{-2} and $R_{ij}^{\text{eq}} = 3.79$ Å.[31] The values of R_{ij}^{eq} between a backbone and a side chain bead appear in Table 1.

The potential energy for angles among three successively connected beads i, j, and k in the nanotubes is described by

$$V_{ijk}^{\text{angle}}(\theta) = \frac{1}{2}K_{ijk}^{\text{angle}}(\cos(\theta) - \cos(\theta_{ijk}^{\text{eq}}))^2 \quad (2)$$

where θ, K_{ijk}^{angle}, and θ_{ijk}^{eq} are the angle, force constant, and equilibrium angle for beads i, j, and k, respectively. Assuming that the cyclic peptide rings are rigid, we use rather high force constants for the angles among three backbone beads. The values of the parameters for the angle potential are $K_{ijk}^{\text{angle}} = 250$ kJ mol $^{-1}$ and $\theta_{ijk}^{\text{eq}} = 135°$ for angles formed by three backbone beads and $K_{ijk}^{\text{angle}} = 50$ kJ mol $^{-1}$ and $\theta_{ijk}^{\text{eq}} = 112.5°$ for angles formed by two backbone and one side chain beads.

The potential energy for dihedral angles formed by four successively connected beads i, j, k, and l is given by

$$V_{ijkl}^{\text{dihedral}}(\theta) = K_{ijkl}^{\text{dihedral}}(1 + \cos(n\theta - \delta_{ijkl})) \quad (3)$$

where θ, $K_{ijkl}^{\text{dihedral}}$, n, and δ_{ijkl} are the dihedral angle, force constant, multiplicity, and phase shift for four successively bonded beads i, j, k, and l, respectively. MD simulations performed by Tarek et al. showed that the cyclic peptide rings are almost flat.[36] To maintain the rings flat, we use rather high force constants for the dihedral angles. The values of the parameters are $K_{ijkl}^{\text{dihedral}} = 100$ kJ mol $^{-1}$, $n = 1$, and $\delta_{ijkl} = 180°$ for a dihedral angle among four backbone beads and $K_{ijkl}^{\text{dihedral}} = 50$ kJ mol $^{-1}$, $n = 1$, and $\delta_{ijkl} = 0°$ for a dihedral angle among three backbones and one side chain bead. No potential is defined for the dihedral angles formed by two backbone beads and two side chain beads.

Nonbonded (nb) interactions between two CG beads i and j are described by the Lennard-Jones (LJ) and Coulomb potentials as

$$V_{ij}^{\text{nb}} = \frac{1}{4\pi\epsilon_r\epsilon_0}\frac{q_i q_j}{r_{ij}} + 4\epsilon_{ij}\left[\left(\frac{\sigma_{ij}}{r_{ij}}\right)^{12} - \left(\frac{\sigma_{ij}}{r_{ij}}\right)^{6}\right] \quad (4)$$

where ϵ_r is a relative dielectric constant ($\epsilon_r = 20$), q_i and q_j are charges for two charged beads i and j, r_{ij} is the distance between two beads i and j, and ϵ_{ij} and σ_{ij} are the LJ potential parameters for the van der Waals (vdW) interaction between two beads i and j. No charges are assigned to any of the CG beads in the cyclic peptide nanotubes, and the charged beads of the lipid molecules are given a charge of $\pm 0.7|e|$. Because the CG beads of the cyclic peptide nanotubes are classified by using the same bead types as for lipid molecules, we can employ the force field of Marrink et al. for the LJ potential parameters of the cyclic peptide nanotube in eq 4 except for the vdw interaction between the nanotube backbone (Nda) and water (P).

For the LJ parameters between the backbone and water, Marrink et al. used an equilibrium distance $\sigma_{ij} = 4.7$ Å and an interaction strength $\epsilon_{ij} = 4.2$ kJ mol $^{-1}$. In our CG MD simulations, we use the same equilibrium distance $\sigma_{ij} = 4.7$ Å, but a different LJ interaction strength $\epsilon_{ij} = 1.8$ kJ mol $^{-1}$ for the backbone-water LJ parameters. CG MD simulations from these modified backbone-water LJ parameters yield a water diffusion coefficient that is close to that from AA MD simulations, as is explained in the next section. Note that the type of backbone bead is still Nda and it interacts with other beads of that type. CG representations of a cyclo[(−D-Ala-L-Glu-D-Ala-L-Gln−)$_2$], a cyclo[(−L-Trp-D-Leu−)$_4$], and a DPPC lipid molecule are shown in Figure 2.

B. Description of the Simulations. The AA MD and CG MD simulations were performed by using NAMD 2.6, while for the CG MD simulations some modifications to NAMD 2.6 were introduced. A cutoff distance of 12 Å was applied to the nonbonded interactions in all simulations. Vdw interactions were smoothly switched to 0 over the range 10 to 12 Å in the AA MD simulations and 9 to 12 Å in the CG MD simulations. In all simulations, Langevin dynamics with a damping coefficient of 5 ps $^{-1}$ was used to maintain temperature. Pair lists were updated every 10 steps with a 20 Å pair list cutoff in all simulations. In AA MD simulations, the CHARMM27 force field and TIP3P water molecules were used to describe the cyclic peptide nanotubes, lipid, and water molecules.

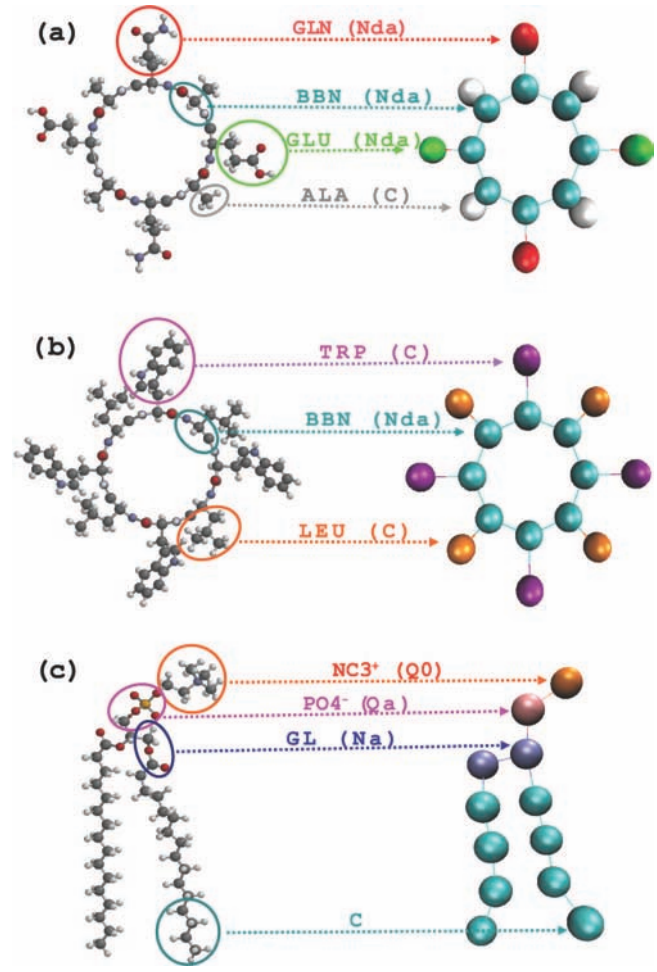

Figure 2. Coarse-grained (CG) representations of cyclic peptide nanotubes: (a) 8 × cyclo[(−D-Ala-L-Glu-D-Ala-L-Gln−)$_2$] and (b) 8 × cyclo[(−L-Trp-D-Leu−)$_4$], and (c) DPPC lipid molecule. BBN in the figure stands for a CG backbone bead of cyclic peptide nanotubes.

1. AA and CG MD Simulations of an 8 × Cyclo[(−D-Ala-L-Glu-D-Ala-L-Gln−)$_2$] Cyclic Peptide Nanotube in Water. Both AA MD and CG MD simulations for an 8 × cyclo[(D-Ala-Glu-D-Ala-Gln)$_2$] cyclic peptide nanotube[1,10] in water were performed with use of the canonical (NVT) ensemble with periodic boundary conditions in all directions. We carried out these simulations to investigate whether the modified CG force field for the cyclic peptide nanotube works well enough to reproduce static and dynamic properties by comparing the results of AA MD and CG MD simulations.

For both AA MD and CG MD simulations, the number of water molecules in the system was calculated on a basis of a partial volume of 0.73 cm^3/g for the nanotube and 1.00 cm^3/g for water.[10,14] In the AA MD simulation, the size of a simulation box is 31.5 Å × 31.5 Å × 62 Å with one cyclic peptide nanotube and 1798 water molecules. An AA MD simulation was carried out for 4 ns at 298 K. The equation of motion was integrated with a time step of 2 fs. After an equilibration of 2 ns, the data were collected and analyzed every 100 fs for another 2 ns.

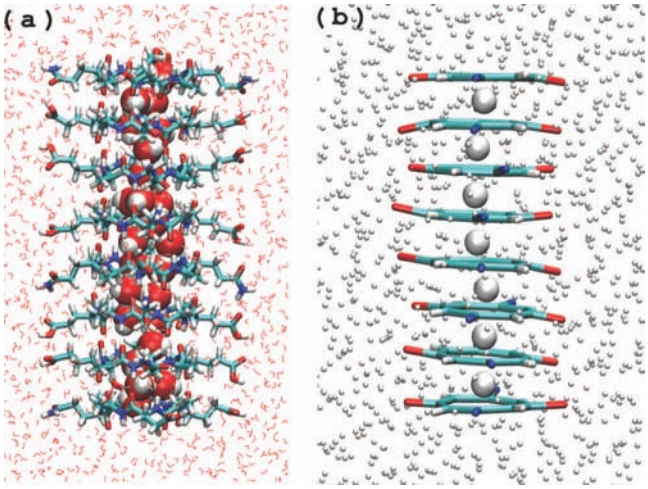

Figure 3. Snapshots from (a) AA and (b) CG MD simulations for an 8 × cyclo[(−D-Ala-L-Glu-D-Ala-L-Gln−)$_2$] in water. Water molecules inside the cyclic peptide nanotubes in both simulations are represented by large VDW spheres, while the other water molecules are described by the line representation.

The system for a CG MD simulation is composed of one CG cyclic peptide nanotube and 4214 CG water molecules in a simulation box that has a dimension of 80.0 Å × 80.0 Å × 80.0 Å. The CG simulation was conducted over a 40 ns interval at 315 K with a time step of 20 fs. The system was equilibrated for 20 ns and the data were collected and analyzed every 1 ps for another 20 ns. Figure 3 shows snapshots from the AA and CG MD simulations.

To compare the calculated features of water that is inside the tube with bulk water, separate AA MD and CG MD simulations in pure water systems were performed at a density of 1.0 g/cm^3 for 2 ns and for 20 ns, respectively.

2. AA and CG MD Simulations of an 8 × Cyclo[(−Trp-D-Leu−)$_4$] in a DPPC Lipid Bilayer. Using the isothermal−isobaric (NpT) ensemble with periodic boundary conditions in all directions, we first performed a CG MD simulation to check whether our CG MD simulations with NAMD 2.6 reproduce the lipid bilayer formation demonstrated by Marrink et al.[18] At the beginning of our simulation, 256 CG DPPC lipid molecules in 3072 CG waters were randomly placed in a simulation box the size of which is 110.0 Å × 110.0 Å × 110.0 Å. The simulation was performed for 80 ns with a time step of 40 fs at 323 K, and the results show the spontaneous bilayer formation shown in Figure 4a.

Next, CG MD simulations in the NpT ensemble with periodic boundary conditions in all directions were carried out to study the insertion of a cyclic peptide nanotube into a DPPC lipid bilayer. The system with an average dimension of 88.8 Å × 88.8 Å × 157.3 Å is composed of one CG 8 × cyclo[(−Trp-D-Leu−)$_4$] nanotube, 256 CG DPPC molecules, and 7500 CG water molecules. A CG DPPC lipid bilayer with 128 CG DPPC lipid molecules in each leaflet was prepared from the previous CG MD simulation for the bilayer formation. For the initial configuration, a CG cyclic peptide nanotube is placed with its center of mass 52.5 Å above the middle of the lipid bilayer (see Figure 4b). Holding the backbones of the nanotube at the initial position with a constraint, the system was equilibrated for 20 ns with a time step of 20 fs. Then, a series of CG simulations were started by lifting the constraint on the nanotube. A constant pressure of 1 atm was maintained by using a Nosé-Hoover Langevin piston method with a piston period of 1000 fs and a decay time of 500 fs. The ratio of simulation box in the $x-y$ plane was kept constant. The CG simulations were carried out at 338 K over 100 ns with a time step of 20 fs.

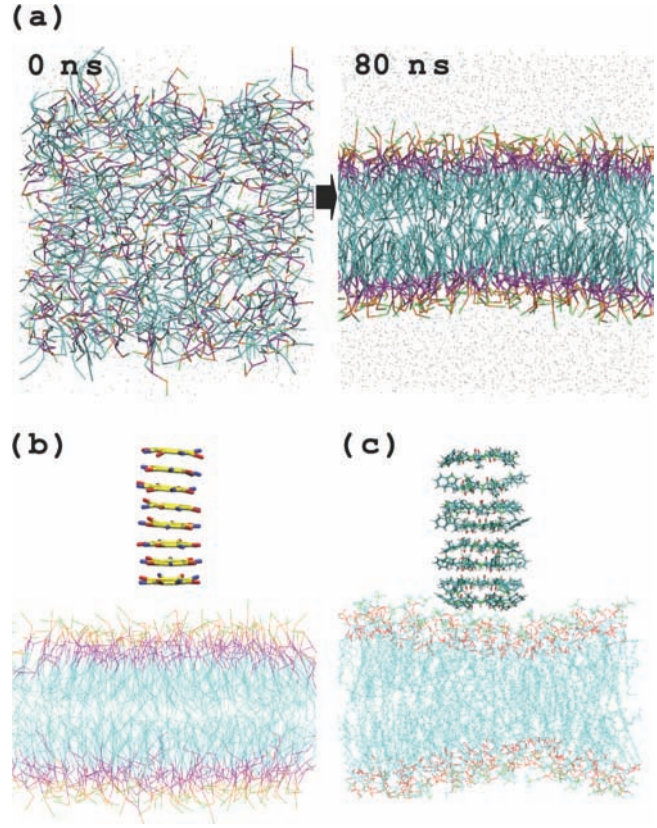

Figure 4. Snapshots from CG and AA MD simulations: (a) a CG MD simulation of self-assembly of lipid molecules into a bilayer from a random distribution after 80 ns, (b) an initial configuration for CG MD simulations of the 8 × cyclo[(−L-Trp-D-LEU−)$_4$] insertion into a CG DPPC lipid bilayer, and (c) an initial configuration for an AA MD simulation of the lipid headgroup insertion into the 8 × cyclo[(−L-Trp-D-LEU−)$_4$]. In parts b and c, water molecules are removed for a better view.

An AA MD simulation in the NpT ensemble with periodic boundary conditions in all directions was also conducted to examine whether a lipid headgroup can be inserted into a cyclic peptide nanotube or not; this will be explained in section III.B. Initially, an 8 × cyclo[(−Trp-D-Leu−)$_4$] nanotube was placed on the top of a DPPC lipid bilayer as shown in Figure 4c. The average size of the AA MD simulation box is 60.0 Å × 60.0 Å × 113.3 Å with one 8 × cyclo[(−Trp-D-Leu−)$_4$] nanotube, 128 DPPC lipid (64 DPPC molecules in each leaflet), and 8157 water molecules. Then, the AA MD simulation is performed over 4 ns with a time step of 1 fs at 323 K. A Nosé-Hoover Langevin piston method with a piston period of 1000 fs and a decay time of 500 fs was used to maintain a constant pressure of 1 atm. As was the case in the CG MD simulations, the ratio of the simulation box dimension in the $x-y$ plane was kept constant. The electrostatic interactions were treated by using the particle mesh Ewald (PME) method with a grid size of 64 × 64 × 128 points.

III. Data and Results

A. AA and CG MD Simulations of an 8 × Cyclo[(−D-Ala-Glu-D-Ala-Gln−)$_2$] Nanotube in Water. To verify our modified and extended CG model, the static and dynamic properties obtained from a CG MD simulation are compared with those from an AA MD simulation. Figure 5a shows the

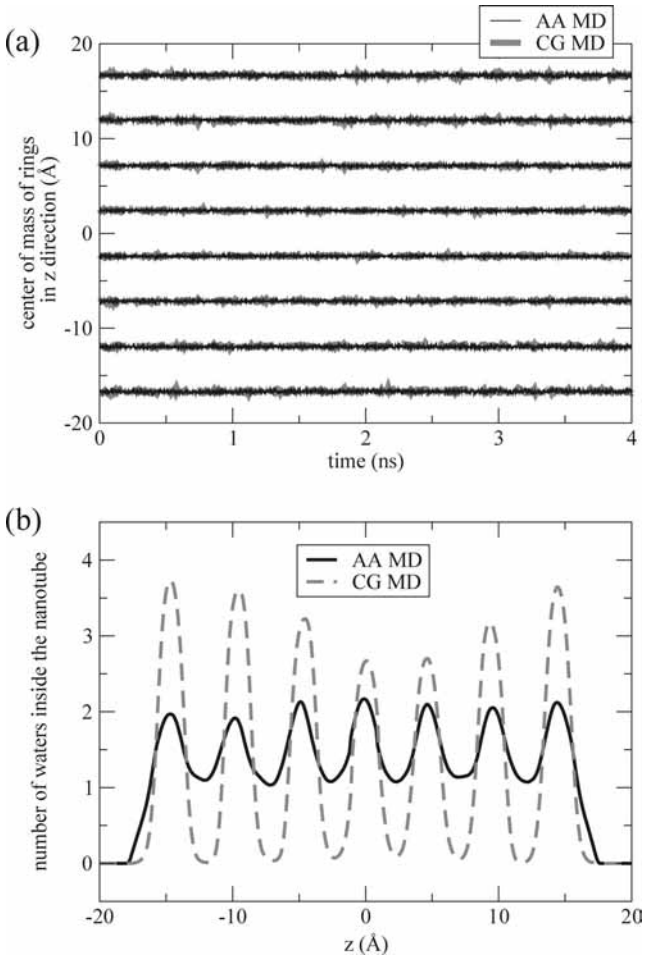

Figure 5. (a) Center of mass of each ring of an 8 × cyclo[(−D-Ala-L-Glu-D-Ala-L-Gln−)$_2$] as a function of time and (b) water density profiles inside the tube obtained from AA and CG MD simulations.

distances between two adjacent cyclic peptide rings as a function of time obtained from the AA and CG simulations. The average distance between two rings is 4.90 Å in both simulations. The average radius of the rings is 4.77 and 4.81 Å in the AA and CG MD simulations, respectively. In the AA and CG MD simulations, hydrogen bonds between adjacent cyclic peptide rings are strong enough that the nanotube maintains a tubular structure in water for a long time. The water density inside the cyclic peptide nanotube as a function of the channel axis coordinate (z) is shown in Figure 5b. An AA MD simulation by Engels et al. indicated that there is typically one water molecule in the plane formed by the eight backbone C $_\alpha$ atoms of a nanotube ring (the α-plane zones) and there are typically two water molecules between two α-plane zones (the midplane zones).[10] The AA MD simulation shows the alternating density of water molecules very well, while the CG water beads in the CG MD simulation are mostly found in the midplane zones because the size of one CG bead representing four water molecules is too large to stay in the α-plane regions. The average numbers of water molecules inside the nanotube are 25.3 and 23.9 for AA and CG MD, respectively, showing good agreement.

To examine whether or not the CG MD simulation reproduces dynamical properties well enough, we calculated the diffusion coefficients of water in the bulk and inside the nanotube from both the AA and CG MD simulations. Figure 6 shows the mean square displacements along the tube axis $\langle \Delta z^2 \rangle$ as a function of time. Using the Einstein−Smoluchowski equation, we obtained the diffusion coefficients along the channel axis in bulk and

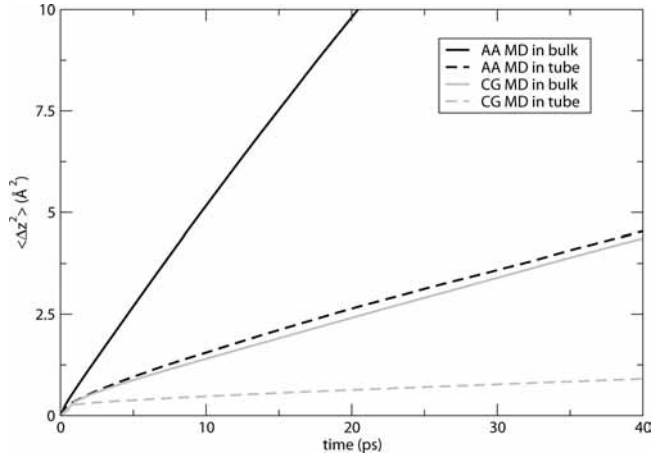

Figure 6. Mean square displacements of water molecules along the tube axis $\langle \Delta z^2 \rangle$ in bulk and inside an 8 × cyclo[(−-D-Ala-L-Glu-D-Ala-L-Gln−)$_2$] tube as a function of time obtained from AA and CG MD simulations. Note that a CG water bead represents four AA water molecules, moving four times as slow as an AA water molecule.

inside the nanotube from the mean square displacement−time curves. Because one CG water bead represents four water molecules, the diffusion coefficient of one CG water bead should be four times slower than that of one water molecule, and the ideal ratio should be 0.25.[18] In bulk, the water diffusion coefficients acquired from the AA and CG MD simulations are 0.228 and 0.0486 Å^2/ps. A ratio of the two diffusion coefficients is 0.0486/0.228 ≈ 0.213, which is very close to the ideal ratio. The water diffusion coefficients inside the tube are 0.0472 and 0.00686 Å^2/ps from the AA and CG MD simulations, respectively. This leads to a ratio of 0.00686/0.0472 ≈ 0.145, which appears to be smaller than the ideal ratio. We can increase the diffusion coefficient of a CG water bead inside the tube by reducing the LJ interaction strength ϵ_{ij} between the nanotube backbone and water beads, that is, by making the backbone more hydrophobic.[37] A problem arising in this case is that the reduced LJ interaction strength between the backbone and water beads results in a smaller number of CG water beads inside the nanotube. After compromising between the inside water density and inside water diffusion coefficient, we chose the value of 1.8 kJ mol $^{-1}$ as the LJ interaction strength between the backbone and water beads. Note that both the AA and CG MD simulation results show that the diffusion coefficient of water inside the nanotube is much smaller than that in bulk. This was also shown by an AA MD simulation by Engels et al.[10]

B. AA and CG MD Simulations for an 8 × Cyclo[(−L-Trp-D-Leu−)$_4$] Nanotube Insertion into a DPPC Lipid Bilayer. We performed a series of CG MD simulations to examine the 8 × cyclo[(−Trp-D-Leu−)$_4$] nanotube insertion into a lipid bilayer. Figure 7 shows snapshots from a CG MD simulation for the cyclic peptide nanotube insertion into the DPPC lipid bilayer. Over a few nanosecond interval, the cyclic peptide nanotube approaches the surface of the bilayer and begins to insert into the lipid bilayer. After insertion, the simulation indicates large fluctuation of the orientation by the nanotube inside the bilayer, but on average it appears to have its long axis parallel to the normal of the bilayer surface. Hydrogen bonding interactions among the cyclic peptide rings is quite strong, so the nanotube is able to maintain the tubular structure both inside and outside the bilayer during the simulation time of 100 ns. This is qualitatively similar to the observations of Kim et al. using Fourier transform infrared (FT-IR) methods, who showed that nanotubes composed of cyclo-

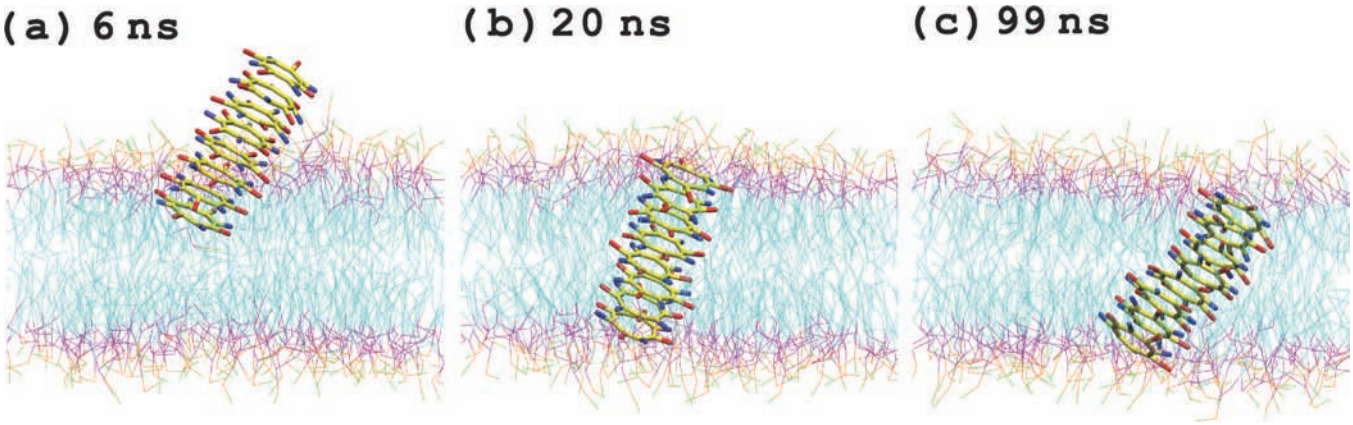

Figure 7. Snapshots of the insertion of an CG 8 × cyclo[(−L-Trp-D-Leu−)$_2$] nanotube into a CG DPPC lipid bilayer at (a) 6, (b) 20s, and (c) 99 ns.

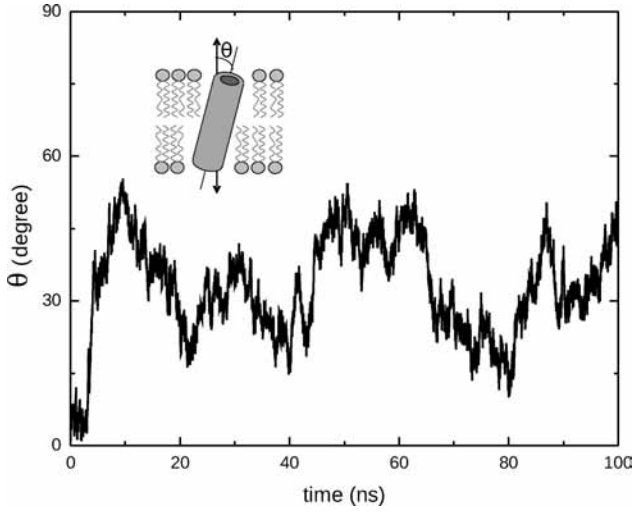

Figure 8. Angle θ as a functions of time for two CG MD simulation trajectories. The angle θ is defined as an angle between the long axis of the tube and the normal of the bilayer plane.

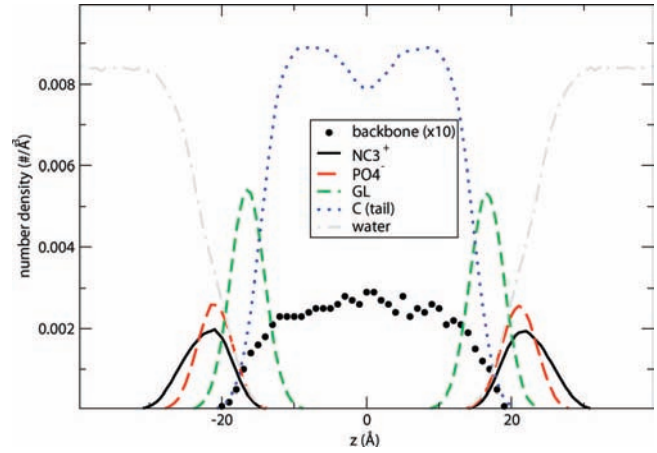

Figure 9. Density profiles of the CG tube backbone, lipid head and tail groups, and water beads. The density of the nanotube backbones was plotted with values ten times as large as its original ones for clarity.

[(−L-Trp-D-Leu−)$_3$-L-Gln-D-Leu−] are aligned parallel to the hydrocarbon chains of the dimyristoyl phosphatidylcholine (DMPC) lipid bilayer.[5]

The CG MD simulation shows that the long axis of the nanotube in the final structures is not exactly normal to the bilayer surface, but tilted at an angle. This tilt structure was also indicated in experiments and AA MD simulations.[5,36] The FT-IR measurements of Kim et al. revealed that the axis of the nanotube is tilted by an angle of 39° with respect to the bilayer normal.[5] This tilt structure of the cyclic peptide nanotube inside a lipid bilayer was confirmed by Tarek and co-workers.[36] Using MD simulations, Tarek et al. showed that the average angle between the amide moiety of a cyclic peptide nanotube and the lipid membrane normal is 25° . We calculated the tilt angle θ between the long axis of the nanotube and the z axis of the simulation box. The long axis of the nanotube was obtained by a moment of inertia tensor analysis of the CG backbone beads. Figure 8 shows the angle as a function of time from the CG MD simulation. There is a considerable fluctuation, indicating reorientation of the nanotube after insertion. The mean value of the angle obtained by averaging from 20 to 100 ns is 34.2°, which agrees well with the FT-IR experiment by Kim et al. and the AA MD simulation by Tarek and co-workers. We propose that the tilt structure of the cyclic peptide nanotube inside the lipid bilayer arises from unfavorable interactions between the hydrophilic lipid head groups and the hydrophobic side chains of the nanotube.[34] The origin of the tilt structure can be further investigated by calculating the potential of mean force of the cyclic nanotube inside the bilayer as a function of angle θ.

Density profiles of the backbone beads of the CG nanotube, the CG lipid head and tail groups, and the CG water molecules are presented in Figure 9. Due to the tilt structure of the nanotube inside the bilayer, the backbones are found in the inner part of the bilayer, suggesting that there are more interactions between the nanotube backbones and the phosphate (PO_4^-) groups than the choline (NC_3^+) groups. This makes sense because the phosphate group, a hydrogen bond acceptor, can participate in hydrogen bonding interactions with the backbones of the nanotube, while the choline group, neither hydrogen bond donor nor acceptor, cannot make any hydrogen bonds with the backbones.

A process that we observe from CG MD simulations during the insertion of the cyclic peptide nanotube into the bilayer is the transfer of a lipid from one leaflet to the other leaflet of the bilayer, so-called lipid flip-flop.[21,32,38] Figure 10 shows a lipid flip-flop induced by the nanotube insertion into the bilayer. This lipid flip-flop occurring in our simulation is possibly caused by hydrophobic interactions between the lipid tails and the side chains of the nanotube and hydrophilic interactions between the lipid heads and the backbone of the cyclic peptide nanotube. Once the insertion of the nanotube is complete, the flipped lipid detaches from the nanotube and diffuses laterally. A lipid flip-

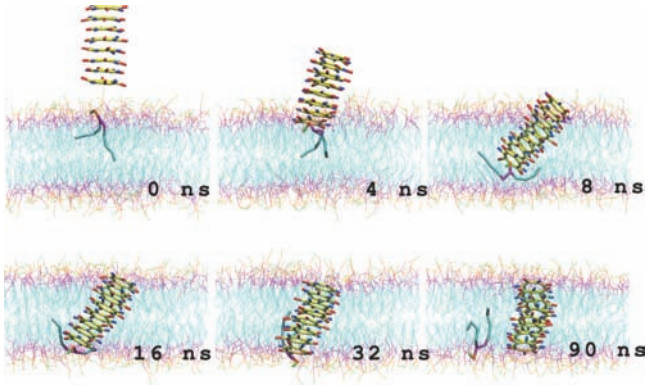

Figure 10. Snapshots of a CG lipid flip-flop induced by the nanotube insertion. The nanotube and flipped lipid are represented by the licorice drawing method, while the other lipid molecules are by the line drawing method.

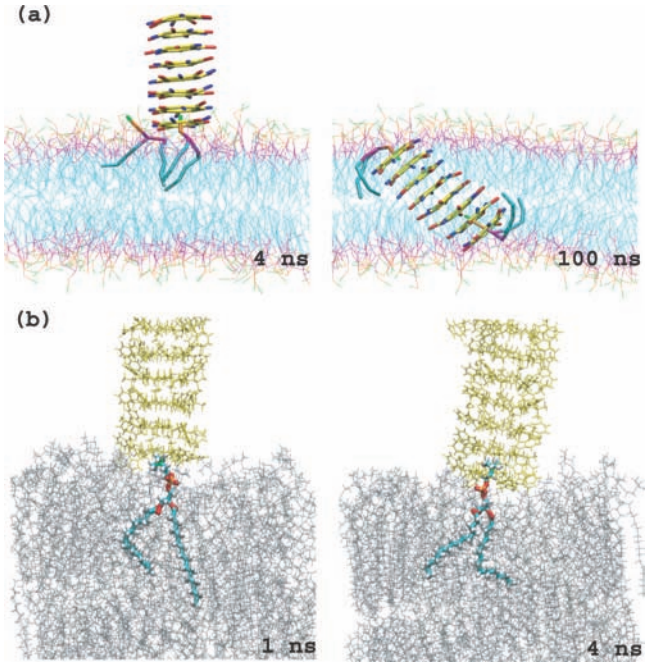

Figure 11. Snapshots of insertions of one or two lipid molecules into the cyclic peptide nanotube shown by (a) CG MD and (b) AA MD simulations. Note that there are two lipids inserting into the nanotube in part a.

flop was also observed in CG MD simulations by Lopez et al. and by Smeijers et al. for a tubular protein insertion into a lipid bilayer.[21,32]

Another observation made from another CG MD simulation is insertions of lipid head groups into the cyclic peptide nanotube shown in Figure 11a. When the nanotube approaches a leaflet of the bilayer, the headgroup of a lipid molecule in that leaflet suddenly inserts into an entrance of the nanotube, and a transfer of the lipid takes place. After the nanotube insertion is complete with the lipid headgroup inside, the headgroup of another lipid molecule can insert into the other entrance of the nanotube. By blocking one or both entrances of the nanotube, this lipid headgroup insertion could prevent a cyclic peptide nanotube from functioning as an ion channel. A CG MD simulation study by Lopez et al. reported an insertion of a lipid tail into a tubular protein.[22] To check the reliability of the CG MD simulation, we also performed an AA MD simulation as described in subsection II.B.2, where an 8 × cyclo[(−L-Trp-D-Leu−)$_4$] nanotube is place on the top of a DPPC lipid bilayer. The 4 ns AA MD simulation indeed shows that a lipid head in the bilayer can hop and insert into the cyclic peptide nanotube. This AA MD simulation is not long enough to show complete insertion, but it demonstrates the reliability of the CG MD simulations we have conducted. One possible driving force of the lipid headgroup insertion into the cyclic peptide nanotube in our simulation is hydrophilic interactions between the backbones of the cyclic peptide nanotube and the lipid head groups, while a possible driving force for lipid tail insertion into a tubular protein in the CG MD simulation by Lopez et al. is interaction of the hydrophobic backbone of the tubular protein with the hydrophobic lipid tails.

IV. Concluding Remarks

We have modified and extended CG models of proteins and lipid molecules for MD simulations to study whether or not a cyclic peptide nanotube can insert into a lipid bilayer and function as an ion channel.

To validate the CG model, we performed both AA and CG MD simulations for a cyclic peptide nanotube with hydrophilic side chains in water and compared the two simulation results. Compared with the AA MD simulation, the CG MD simulation reproduces the static and dynamic properties very well. Static properties obtained from the CG MD simulation, like the average distance between two adjacent rings, average ring size, and water density inside the nanotube, show good agreement with those from the AA MD simulation. Diffusion coefficients inside the tube as well as in bulk from the CG MD simulation also show reasonable agreement with the AA MD results.

The CG MD simulations performed with a cyclic peptide nanotube with hydrophobic side chains showed that the nanotube can insert into a DPPC lipid bilayer with its long axis normal to the bilayer surface, leading to at least the possibility that the tube will function as an ion channel. Hydrogen bonds connecting two cyclic peptide rings are so strong that the nanotube is able to maintain the tubular structure of the nanotube over the simulation time of 100 ns.

According to our CG MD simulations, although the long axis of the nanotube is approximately normal to the bilayer plane, it is not completely perpendicular, but is tilted at an angle. This tilt structure of the nanotube inside a lipid bilayer was also confirmed by an FT-IR experiment and an AA MD simulation. The calculated angle as a function of time shows that the orientation of the nanotube is fluctuating around the average tilt angle. We propose that the tilt structure of the cyclic peptide nanotube inside a lipid bilayer originates from unfavorable interactions between the hydrophilic lipid head groups and hydrophobic side chains of the nanotube.

The density profiles of the backbone beads of the nanotube suggest that there are more interactions between the nanotube backbones and the phosphate (PO_4^-) groups than the choline (NC_3^+) groups. This is supported by the fact that the phosphate in a lipid headgroup is a hydrogen bond acceptor, and can participate in hydrogen bond interactions with the backbones of the nanotube, while the choline group, neither hydrogen bond donor nor acceptor, cannot make any hydrogen bonds with the backbones.

A lipid flip-flop process induced by nanotube insertion was observed from our CG MD simulation. After the lipid flip is completed, the lipid detaches from the nanotube and diffuses laterally. From the simulation, we suggest that a driving force for the lipid flip-flop is hydrophobic interactions between the side chains of the nanotube and lipid tail groups and hydrophilic

interactions between the backbone of the nanotube and lipid head groups.

This CG MD simulation study also revealed insertions of lipid head groups into the cyclic peptide nanotube; this was also confirmed by an AA MD simulation in this study. This lipid headgroup insertion into the nanotube could prevent a cyclic peptide nanotube from functioning as an ion channel by blocking the channel.[8] Our finding suggests that special care should be taken when a cyclic peptide ring is synthesized with a larger number of amino acid residues.[7]

In this study, we did not make a thorough discussion of the origins of the tilt structure of the cyclic peptide nanotubes inside the bilayer. The origin of the tilt structure is one of the main issues in protein and peptide insertion into cell membranes,[21,31,39] and can be examined by calculating a potential of mean force of the nanotube inside the lipid bilayer as a function of the angle between the long axis of the nanotube and the bilayer normal.[40] Another issue associated with the tilt structure is hydrophobic mismatch, the dependence of the tilt angle on the length of the nanotube, which can be explored by changing the number of the cyclic peptide rings forming the nanotube.[34] Although it was confirmed by an AA MD simulation, insertion of the lipid head groups into the cyclic peptide nanotube by our CG MD simulations should be more carefully examined because that process strongly depends on the CG force fields.

Acknowledgment. G.C.S. and H.H. were supported by NSF grant CHE-0550497, by the Northwestern Center for Cancer Nanobiotechnology Excellence (1 U54 CA 119341-01), and by the Network for Computational Nanotechnology.

References and Notes

(1) Ghadiri, M. R.; Granja, J. R.; Milligan, R. A.; McRee, D. E.; Khazanovich, N. *Nature* **1993**, *366*, 324.
(2) Ghadiri, M. R.; Granja, J. R.; Buehler, L. K. *Nature* **1994**, *369*, 301.
(3) Ghadiri, M. R.; Kobayashi, K.; Granja, J. R.; Chadha, R. K.; McRee, D. E. *Angew. Chem., Int. Ed. Engl.* **1995**, *34*, 93.
(4) Motesharei, K.; Ghadiri, M. R. *J. Am. Chem. Soc.* **1997**, *119*, 11306.
(5) Kim, H. S.; Hartgerink, J. D.; Ghadiri, M. R. *J. Am. Chem. Soc.* **1998**, *120*, 4417.
(6) Hartgerink, J. D.; Clark, T. D.; Ghadiri, M. R. *Chem. Eur. J.* **1998**, *4*, 1367.
(7) Sánchez-Quesada, J.; Kim, H. S.; Ghadiri, M. R. *Angew. Chem., Int. Ed.* **2001**, *40*, 2503.
(8) Fernadez-Lopez, S.; Kim, H. S.; Choi, E. C.; Delgado, M.; Granja, J. R.; Khasanov, A.; Kraehenbuehl, K.; Long, G.; Weinberger, D. A.; Wilcoxen, K. M.; Ghadiri, M. R. *Nature* **2001**, *412*, 452.
(9) Horne, W. S.; Wiethoff, C. M.; Cui, C. L.; Wilcoxen, K. M.; Amorin, M.; Ghadiri, M. R.; Nemerow, G. R. *Bioorg. Med. Chem.* **2005**, *13*, 5145.
(10) Engels, M.; Bashford, D.; Ghadiri, M. R. *J. Am. Chem. Soc.* **1995**, *117*, 9151.
(11) Smith, G. R.; Sansom, S. P. *Biophys. J.* **1998**, *75*, 2767.
(12) Allen, T. W.; Kuyucak, S.; Chung, S.-H. *Biophys. J.* **1999**, *77*, 2502.
(13) Allen, T. W.; Andersen, O. S.; Roux, B. *Proc. Natl. Acad. Sci. U.S.A.* **2004**, *101*, 117.
(14) Hwang, H.; Schatz, G. C.; Ratner, M. A. *J. Phys. Chem. B* **2006**, *110*, 6999.
(15) Shelly, J. C.; Shelly, M. Y.; Reeder, R. C.; Bandyopadhyay, S.; Klein, M. L. *J. Phys. Chem. B* **2001**, *105*, 4464.
(16) Shelly, J. C.; Shelly, M. Y.; Reeder, R. C.; Bandyopadhyay, S.; Moore, P. B.; Klein, M. L. *J. Phys. Chem. B.* **2001**, *105*, 9785.
(17) Stevens, M. J. *Phys. Rev. Lett.* **2003**, *91*, 188102.
(18) Marrink, S. J.; de Vries, A. H.; Mark, A. E. *J. Phys. Chem. B* **2004**, *108*, 750.
(19) Nielsen, S. O.; Lopez, C. F.; Srinivas, G.; Klein, M. L. *J. Phys.: Condens. Matter* **2004**, *16*, R481.
(20) Nielsen, S. O.; Ensing, B.; Ortiz, V.; Moore, P. B.; Klein, M. L. *Biophys. J.* **2005**, *88*, 3822.
(21) Lopez, C. F.; Nielsen, S. O.; Moore, P. B.; Klein, M. L. *Proc. Natl. Acad. Sci.* **2004**, *101*, 4431.
(22) Lopez, C. F.; Nielsen, S. O.; Ensing, B.; Moore, P. B.; Klein, M. L. *Biophys. J.* **2005**, *88*, 3083.
(23) Markvoort, A. J.; Pieterse, K.; Steijaert, M. N.; Spijker, P.; Hilbers, P. A. J. *J. Phys. Chem. B* **2005**, *109*, 22649.
(24) Izvekov, S.; Voth, G. A. *J. Phys. Chem. B.* **2005**, *109*, 2469.
(25) Shi, Q.; Voth, G. A. *Biophys. J.* **2005**, *89*, 2385.
(26) Venturoli, M.; Smit, B.; Sperotto, M. *Biophys. J.* **2005**, *88*, 1778.
(27) Venturoli, M.; Sperotto, M. M.; Kranenburg, M.; Smit, B. *Phys. Rep.* **2006**, *437*, 1.
(28) Lee, H.; Larson, R. G. *J. Phys. Chem. B* **2006**, *110*, 18204.
(29) Shih, A. Y.; Arkhipov, A.; Freddolino, P. L.; Schulten, K. *J. Phys. Chem. B* **2006**, *110*, 3674.
(30) Shih, A. Y.; Freddolino, P. L.; Arkhipov, A.; Schulten, K. *J. Struct. Biol.* **2007**, *157*, 579.
(31) Bond, P. J.; Sansom, M. S. P. *J. Am. Chem. Soc.* **2006**, *128*, 2697.
(32) Smeijers, A. F.; Pieterse, K.; Markvoort, A. J.; Hilbers, P. A. J. *J. Phys. Chem. B* **2006**, *110*, 13614.
(33) Shi, Q.; Izvekov, S.; Voth, G. A. *J. Phys. Chem. B* **2006**, *110*, 15045.
(34) Monticelli, L.; Kandasamy, S. K.; Periole, X.; Larson, R. G.; Tieleman, D. P.; Marrink, S. J. *J. Chem. Theory Comput.* **2008**, *4*, 819.
(35) Treptow, W.; Marrink, S.-J.; Tarek, M. *J. Phys. Chem. B* **2008**, *112*, 3277.
(36) Tarek, M.; Maigret, B.; Chipot, C. *Biophys. J.* **2003**, *85*, 2287.
(37) Brovchenko, I.; Geiger, A.; Oleinikova, A.; Paschek, D. *Eur. Phys. J. E* **2003**, *12*, 69.
(38) Kol, M. A.; van Laak, A. N. C.; Rijkers, D. T. S.; Killian, J. A.; de Kroon, A. I. P. M.; de Kruijff, B. *Biochemistry* **2003**, *42*, 231.
(39) Kandasamy, S. K.; Larson, R. G. *Biophys. J.* **2006**, *90*, 2326.
(40) Lee, J.; Im, W. *Phys. Rev. Lett.* **2008**, *100*, 018103.

JP8080657